Quaternary Geochronology 48 (2018) 171–179

Contents lists available at ScienceDirect

Quaternary Geochronology

journal homepage: www.elsevier.com/locate/quageo

Chronology of a late Neolithic site along the coast of the east China sea

Jianhui Jin[a,b,*], Zhizhong Li[a,b,**], Yunming Huang[c], Xuechun Fan[c], Feng Jiang[b,e], Yan Cheng[b], Xiaolin Xu[b], Zhiyong Ling[d], Xiuming Liu[a,b,f]

[a] Institute of Geography, Fujian Normal University, Fuzhou, 350007, China
[b] Key Laboratory for Humid Subtropical Eco-geographical Processes of the Ministry of Education, Fujian Normal University, Fuzhou, 350007, China
[c] Institude of Archaeology, Fujian Provincial Museum, Fuzhou, 350001, China
[d] Qinghai Institude of Salt Lakes, Chinese Academy of Sciences, Xi'ning, 810008, China
[e] State Key Laboratory of Estuarine and Coastal Research, East China Normal University, Shanghai, 200062, China
[f] Department of Environment and Geography, Macquarie University, NSW 2109, Australia

ARTICLE INFO

Keywords:
Pingfengshan site
Coastal area
Optically stimulated luminescence dating
Neolithic shell mound
Huangguashan culture
South China

ABSTRACT

Shell mounds are the foremost type of Neolithic sites found in coastal areas of South China. These sites can provide significant information on prehistoric human activity and climate change; however, only a few shell mounds have a systematic chronology in South China. In this study, optically stimulated luminescence (OSL) and ^{14}C dating techniques were employed to establish a systemic chronological framework for a Neolithic shell mound found at Pingfengshan in the coastal area of Fujian Province, southern China. In addition, the possible reasons for human coastal migrations that took place during this specific period, along with their associations with climate change, are discussed. The results showed that the obtained OSL ages were reliable and consistent with the ^{14}C chronology. The age of the Pingfengshan site was found to be approximately 4.0–3.3 ka. Additionally, it was found that post-depositional anthropogenic disturbances can have various influences on the resultant OSL and ^{14}C ages. Cross-validation between different dating methods proved to be of great importance to adequately determine the chronology in archaeological sites. The study revealed that climatic changes played a crucial role in prehistoric human migration during the Huangguashan cultural period (4.3–3.2 ka). Sea level fluctuation may have affected onshore living space and site selection of prehistoric settlements, and intensive winter monsoons may have caused the recession of the Huangguashan culture.

1. Introduction

Chronology is crucial for both archaeological and palaeoenvironmental research (Kitis and Vlachos, 2013). In recent years, numerous studies, using reliable dating techniques, have been conducted at Neolithic sites to reconstruct past sedimentary processes (Mischke et al., 2017), palaeoclimatic conditions (Jin et al., 2016; Nian et al., 2015), and human-environmental interactions in China (Sun et al., 2017). This research has been especially important in the Tibetan Plateau and North China, and has even been used to address controversial problems, such as human adaptation (Chen et al., 2015; Sun et al., 2017) and anthropogenesis (Li et al., 2017).

Two dating methods, namely optically stimulated luminescence (OSL) and ^{14}C dating, are considered suitable for archaeological sites with different sedimentary facies, especially for aeolian sediments (Yu et al., 2016). Most recently, Sun et al. (2017) dated 14 hearths at the Yandongtai and Bronze Wire sites in the northeast part of the Qinghai Lake area. There was a good agreement between OSL dating results and charcoal ages during the last deglaciation period, which indicates that the OSL method has great potential in dating hearths on the Qinghai-Tibetan Plateau (ChongYi et al., 2015). Jin et al. (2017) dated the Anshan cultural layer southeast of Fujian Province, and obtained OSL ages from 6.1 ± 0.52 to 1.7 ± 0.12 ka, thereby confirming the stratigraphic sequence with the corresponding AMS ^{14}C age of shells on the top of the layer (1340 ± 35 a BP). These studies showed that OSL dating and AMS ^{14}C dating were in agreement within error and offered reliable chronologies for these sites. Nevertheless, in some practical applications, the results of OSL and ^{14}C dating are affected by different factors and are often inconsistent. This could be a result of post-depositional anthropogenic disturbance, which can influence OSL and ^{14}C ages differently (Yu et al., 2016). For instance, the OSL ages of the Yutian site, in the north-western margin of the Qinghai-Tibetan Plateau,

* Corresponding author. Institute of geography, Fujian normal university, Fuzhou, Fujian, 350007, China.
** Corresponding author. Institute of geography, Fujian normal university, Fuzhou, Fujian, 350007, China.
E-mail addresses: geojjh@fjnu.edu.cn (J. Jin), lizz@fjnu.edu.cn (Z. Li).

https://doi.org/10.1016/j.quageo.2018.10.001
Received 1 August 2017; Received in revised form 27 July 2018; Accepted 3 October 2018
Available online 09 October 2018
1871-1014/ © 2018 Published by Elsevier B.V.

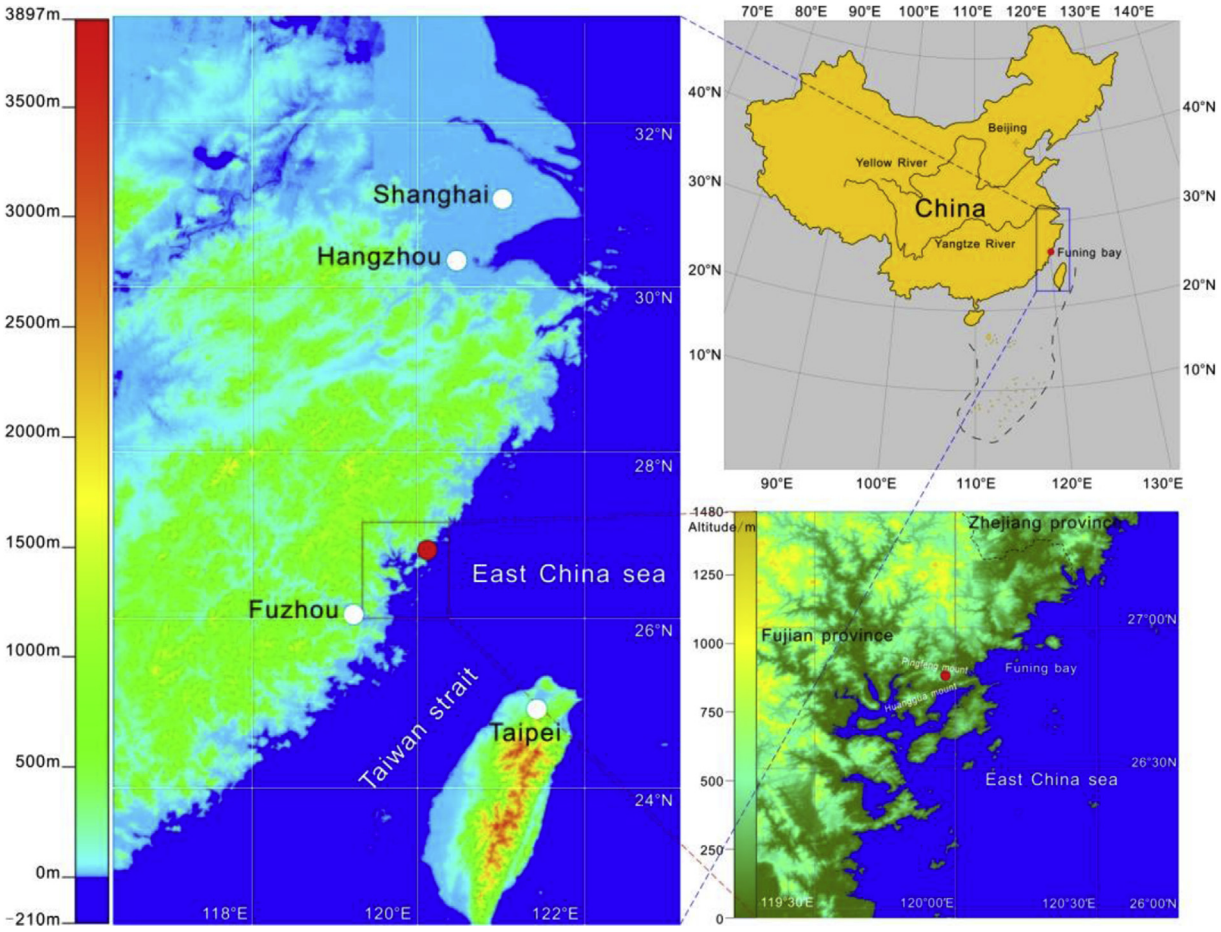

Fig. 1. Geomorphology of the study region and location of the section. The red dot represents the Pingfengshan site location. DEM (digital elevation model) data were downloaded from the Consortium for Spatial Information (http://srtm.csi.cgiar.org/SELECTION/inputCoord.asp), and the map features were modified by CorelDraw 12.

were systematically older than the ^{14}C ages (Han et al., 2017). Further, there are several Neolithic sites lacking reliable charcoal material because of chemical weathering over a long period under hot and humid conditions in the low latitudes of China. Therefore, a comparison between OSL and ^{14}C ages is crucial for resolving potential uncertainty, as long as it is possible to obtain dating material for both OSL and ^{14}C dating of the same formation at a site.

Although the East China Sea coastal area has long been regarded as a crucial region for Neolithic archaeological research (Rolett et al., 2011; Zheng et al., 2009), the Fujian coast has received much less attention, and high-resolution studies of this area are rare (Jin et al., 2017). A Neolithic site on the hilltop of the Pingfengshan mount, about 2 km away from the East China Sea rim (Fig. 1), was recently found and excavated. Stone tools, bone implements, pottery, protoporcelain, millet, and charcoal were associated with the site, thereby providing an opportunity to precisely date these remains and understand the cultural change in the region and the climatic conditions that followed this transformation. This study aimed to fill the gap in our knowledge of the chronology of Neolithic southeast China. Here, we applied OSL and ^{14}C dating to create a systemic chronological framework for this Neolithic site, and discussed the possible reasons for the human coastal migrations that occurred during this specific period, in addition to their associations with climate change.

2. Study area

Fujian Province, located in southeast China opposite the island of Taiwan and separated by the Taiwan Strait (Fig. 1), played an important role in the Neolithic settlement of South China. The terrain features of Xiapu County, located in the northeast of Fujian Province, are characterised by narrow coastal plains, hills, offshore islands, and ocean bays. The Huangguashan Neolithic culture is of significance here, as; it flourished between 4300 and 3200 ka (relative to AD 1950) along the narrow coastal plains and ocean bays of eastern Fujian (Fan et al., 2017).

The Pingfengshan site (26°48′37.89″N, 119°59′45.37″E) is situated atop a mountain near the east coast of Xiapu County in Fujian Province, about 163 m above sea level and roughly 8 km to the northeast of the Huangguashan site (Fig. 1c). A small-scale excavation was conducted in 2016 on the north slope of the mountain (Fig. 2). Taking the west profile of the excavation unit as an example, the site formation can be divided into five groups. Layer 1 was about 5–15 cm thick, where some modern remains and pottery were unearthed. Layer 2, about 10–25 cm in thickness, was characterised by a grey-yellow colour and contained a small amount of protoporcelain. The third layer contained a small quantity of pottery and protoporcelain, and reached a maximum thickness of 55 cm. There were abundant shells, sherds of pottery, and animal bones, along with a small quantity of carbon bits and pellets of burnt soil unearthed from Layers 4 and 5. The emergence of a red weathering crust under Layer 5 indicated the end of the cultural stratigraphic accumulation.

More than 1500 sherds of pottery were unearthed from the Pingfengshan site, but no pottery, after repair, access to complete artefacts restoration. The types of pottery sherds mainly consisted of sandy pottery, clay pottery, hard pottery, black pottery, and painted pottery. According to the decorative patterns and shapes of the artefacts

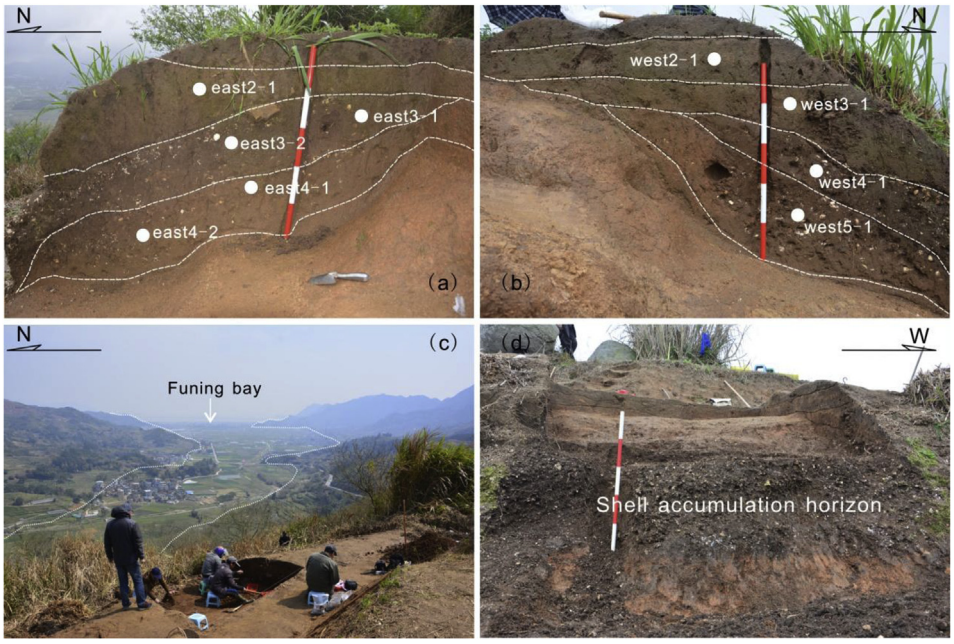

Fig. 2. Profile characteristics and the geomorphological position of the excavation site. (a) The east profile of the excavation site and OSL sampling location. (b) The west profile of the excavation site and OSL sampling location. (c) The geomorphological position of the excavation site, opposite Funing Bay and located on Pingfengshan hill. (d) The shell accumulation horizon of this site.

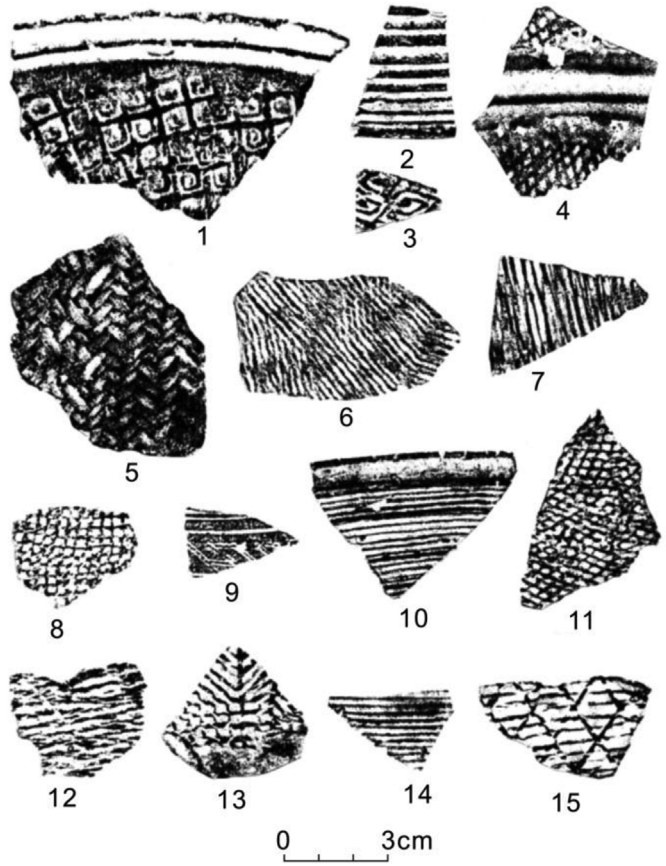

Fig. 3. The pottery emblazonment. The major emblazonment was plain-looking, and a small portion of the pottery was decorated with different patterns, such as Yun-lei (cloud and thunder) veins (No. 1, 3, and 9), rope veins (No. 6, 7, and 12), basket veins (No. 5 and 13), string veins (No. 2, 10, and 14), diamond-striped veins (No. 15), and chequered veins (No. 4, 8, and 11).

excavated from this site (Fig. 3), the primary represented material was from the end of the Huangguashan Period (Fan et al., 2017).

3. Methods

3.1. Sampling

As a dating method, OSL has been revolutionised since the early 2000s (Wintle and Murray, 2006), and can be applied to estimate the depositional or burial age of sediments in a variety of sedimentary environments (Aitken, 1998). Therefore, quartz OSL signals were employed to determine the age of the OSL samples. To check the accuracy of the OSL data used in this study, ^{14}C samples were also collected from the same layers as the OSL samples. Charcoal and rice remains were collected for ^{14}C dating.

Nine OSL samples and seven ^{14}C samples were collected to provide a chronological framework for the Pingfengshan site, and the approximate positions of each OSL sample are shown as white filled circles in Fig. 2a and b. The ^{14}C samples collected from the cultural layers were collected as a single block and wrapped with aluminium foil, and the OSL samples from different layers were collected and wrapped with a stainless steel tube and plastic tape to provide protection against light and breakage during transportation.

3.2. OSL dating

An automated RisØ TL/OSL-DA-20CD reader, equipped with a $^{90}Sr/^{90}Y$ beta source, was used for the measurements in the Fujian Normal University laboratory. The signal was stimulated by blue diodes ($\lambda = 470 \pm 20$ nm) at 130 °C for 40 s, and a Hoya U-340 (7.5 mm) filter, placed in front of the photomultiplier tube, was used for detection.

The single aliquot regenerative dose protocol was used for the quartz OSL measurements (Murray and Wintle, 2000). Medium-grained (38–63 μm) quartz was extracted for equivalent dose (D_e) determination, which was estimated by interpolation of the natural luminescence signal onto the growth curve. The growth curves of these samples were built using regeneration doses, including a zeroth dose for monitoring the thermal transfer effect and a repeated first regeneration dose for checking the accuracy of the sensitivity correction. A fixed, small test dose after the natural and regenerative OSL measurements was used to

Table 1
Summary of U, Th, and K contents, dose rates, D_e values, and OSL ages for the Neolithic site.

Lab code	Sample ID	K (%)	Th (ppm)	U (ppm)	Total dose rate (Gy/ka)	D_e (Gy)	Age (ka)
FNU2016001	West Layer 2-1	3.04 ± 0.07	35.5 ± 0.85	8.27 ± 0.20	6.95 ± 0.32	3.26 ± 0.07	0.47 ± 0.02
FNU2016002	West Layer 3-1	2.75 ± 0.07	28.2 ± 0.68	7.65 ± 0.19	6.08 ± 0.28	9.51 ± 0.17	1.56 ± 0.08
FNU2016003	West Layer 4-1	2.46 ± 0.06	30.4 ± 0.73	6.78 ± 0.18	5.75 ± 0.63	19.42 ± 0.20	3.38 ± 0.37
FNU2016004	West Layer 5-1	2.48 ± 0.06	27.5 ± 0.66	6.83 ± 0.18	5.58 ± 0.26	22.33 ± 0.26	4.00 ± 0.19
FNU2016005	East Layer 2-1	2.81 ± 0.07	29.4 ± 0.71	6.79 ± 0.18	5.97 ± 0.28	3.36 ± 0.10	0.56 ± 0.03
FNU2016006	East Layer 3-1	2.48 ± 0.06	33.6 ± 0.81	7.84 ± 0.20	6.16 ± 0.28	23.54 ± 0.78	3.82 ± 0.22
FNU2016007	East Layer 3-2	2.82 ± 0.07	29.6 ± 0.71	6.80 ± 0.18	6.04 ± 0.28	15.78 ± 0.16	2.61 ± 0.12
FNU2016008	East Layer 4-1	2.78 ± 0.07	33.5 ± 0.80	7.05 ± 0.18	6.28 ± 0.29	21.20 ± 0.21	3.38 ± 0.16
FNU2016009	East Layer 4-2	2.92 ± 0.07	32.2 ± 0.77	6.72 ± 0.17	6.24 ± 0.29	20.60 ± 0.34	3.30 ± 0.16

adjust the sensitivity. The preheat temperature for natural and regenerative doses of samples was 240 °C (for 10 s), and the cut-heat was set at 200 °C for 0 s for test doses in this study. The first 1.6-s integral of the primary OSL signal, minus a background signal estimated from the last 8-s integral, was used for D_e estimation.

The concentrations of U, Th, and K were measured using neutron activation analysis at the China Institute of Atomic Energy. Theoretically, the effect of heterogeneous environmental radionuclide concentrations on the gamma dose rate should be considered due to the finite thickness of cultural layers in archaeological sites. Therefore, samples used for U, Th, and K concentration measurements should include different materials (e.g. charcoals, ash, and seashells, which might lower or contribute to the average concentration of U, Th, and K in sediments) according to the natural volume ratio in different layers. The sampling location should also be considered. For the 38–63 μm quartz grains, an alpha efficiency factor of 0.035 ± 0.003 was assumed so as to estimate the alpha contribution to the dose rate (Lai et al., 2008). The annual dose rates (Aitken, 1998) are shown in Table 1. The long-term water contents were assumed to be 15 ± 5% and were added to each value in the age calculations.

3.3. ^{14}C dating

The ^{14}C samples were mainly collected from the same layers as the OSL samples. Two types of dating materials (charcoals and rice seeds) were collected for use in the ^{14}C dating in this study.

Charcoals are the most frequently used materials for archaeological sites dating (Han et al., 2017). This material is easily affected by old carbon, which originates from the remains of woody plants, such as old dead trees and the wood in ancient buildings or tombs. Thus, the ^{14}C age of this material mainly represents the period of woody material formation rather than human activities. Moreover, the ^{14}C ages from charcoals are easily overestimated due to re-transportation and re-deposition. The relics of crops (rice or millet), which are not commonly found in the archaeological sites of Fujian, are a suitable alternative material for ^{14}C dating. This material avoids the contamination by old carbon and minimises the possibility of re-transportation and re-deposition. Consequently, seeds are ideal material for ^{14}C dating and can offer good age control in archaeological sites.

We chose the most suitable dating samples according to the actual conditions in this study. Finally, 7 AMS ^{14}C samples (charcoal and rice) were selected and measured in the Beta Analytic Radiocarbon Dating Laboratory (Fan et al., 2017) and the Center for Applied Isotope Studies at the University of Georgia (Deng et al., 2017). All radiocarbon dates were calibrated to calendar years (i.e. cal a BP) using the IntCal13 atmospheric curve calibration (Reimer et al., 2013).

4. Results

4.1. Luminescence characteristics and OSL ages

A preheat plateau test was implemented for sample 2016009, which was collected from Layer 4 of the eastern profile of the Pingfengshan site (Fig. 4). Each data point is the mean obtained from four medium-sized aliquots, and the given uncertainty is based on 1 standard error (σ). The results showed that the dose measurement was insensitive to the preheat temperature. No thermal transfer was detected, and the recuperation was less than 3% of the D_e value for the corresponding sample. The dose recovery ratios were close to unity at all preheat temperatures between 180 and 280 °C. The mean recycling ratio generated from each sample's D_e measurement was 1.02 ± 0.03. The CW-OSL signals (Fig. 5) and typical OSL decay curves (Fig. 6) from natural quartz grains showed that the OSL signals were dominated by the fast component. The fast component percentages of the CW-OSL signals from natural quartz grains were more than 70% for all the OSL samples (Fig. 5).

Small aliquots were less influenced by averaging effects and were more effective for identifying grains that were not well bleached before burial (Olley et al., 1999). Therefore, all samples were measured with 2 mm diameter aliquots. The D_e values displayed a tight, normal Gaussian distribution, which suggested that the sediment was sufficiently bleached prior to deposition and that the small aliquots were capable of yielding reliable burial ages for the sediment. All the D_e values were calculated using the central age model, and the resulting 9 OSL ages are summarised in Table 1. The obtained D_e values of the western profile of the excavation site gradually increased with depth, and ranged from 3.26 ± 0.07 to 22.33 ± 0.26 Gy. The OSL ages, which ranged from 0.47 ± 0.02 to 4.00 ± 0.19 ka, were consistent with the stratigraphic order and the depth of the profile. The D_e values and ages of the eastern profile were inconsistent with the stratigraphic sequence. These values could have been affected by the sampling location, human activities, and the form of the land slope (Fig. 2). Therefore, the ages of the cultural accumulation layers (Layers 3 and 4) of the eastern profile were generally focused around 3.3–3.8 ka, which was consistent with the results of the cultural accumulation layers of the western profile.

In addition, the D_e values of the OSL samples obtained from the main Neolithic cultural stratum showed a typical Gaussian distribution, which was characterised by leptokurtic kurtosis and smaller relative errors (Fig. 6a, b, and c). The growth curves of these samples were fitted using a single exponential equation. The calculated D_e values of all samples were smaller than their $2D_0$ values, thereby suggesting that the OSL signals were not saturated (Table 1).

4.2. AMS ^{14}C ages

Information and ages for all samples are listed in Table 2, as well as in Fig. 7. The final ^{14}C dates of charcoal ranged from 3.26 ± 0.03 to 3.40 ± 0.03 ka. The ^{14}C dates of rice, which ranged from 3.35 ± 0.03 to 3.44 ± 0.03 ka, were in agreement with the stratigraphic order as a whole.

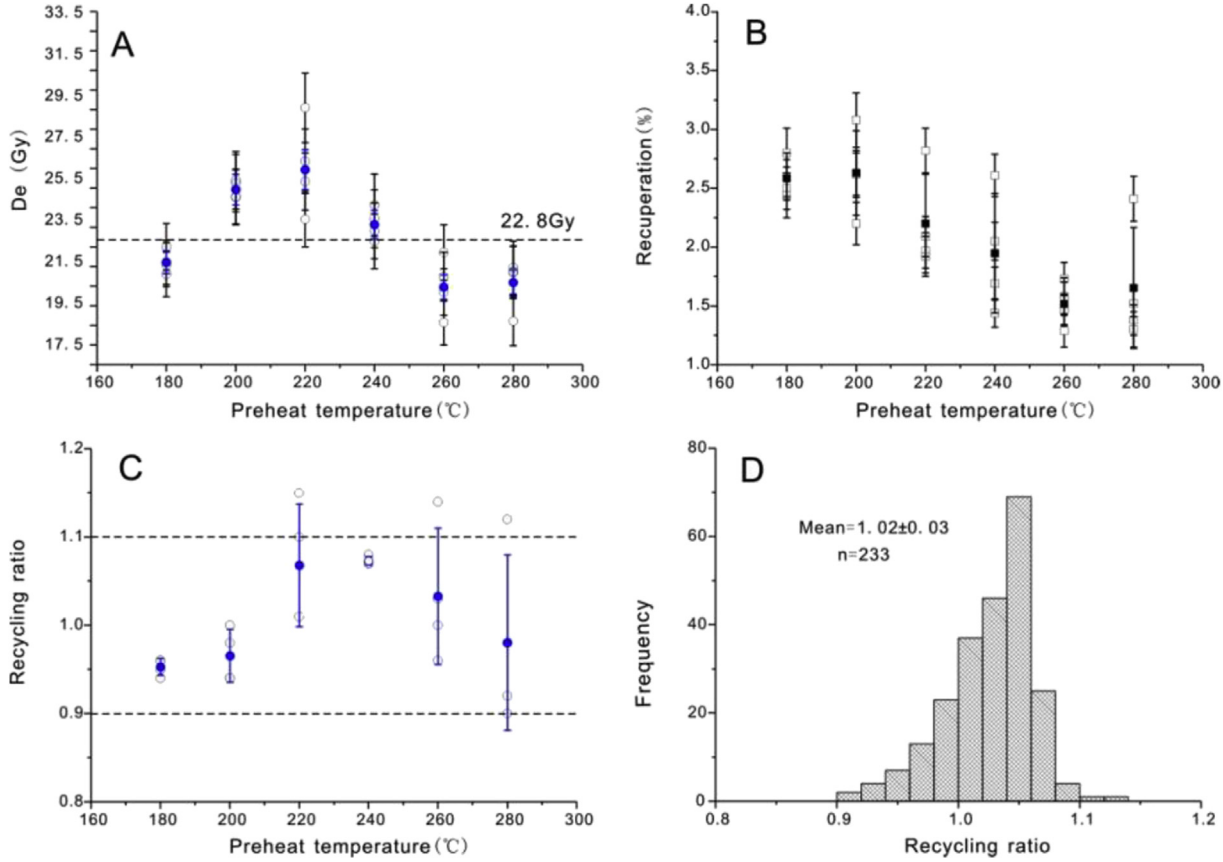

Fig. 4. Results from the preheat plateau test of sample 2016009. (a) Solid circles display the equivalent dose as a function of the preheat temperature for medium-grained quartz. Four aliquots were measured at each temperature, and the error bars represent 1 standard error. The dashed line is drawn at the average D_e value over the 180–280 °C interval. (b) Solid squares present the average recuperation at intervals of 20 °C. (c) The dashed lines are drawn at ± 10%. (d) Histogram of the recycling ratios for all samples (measured as part of the D_e determination).

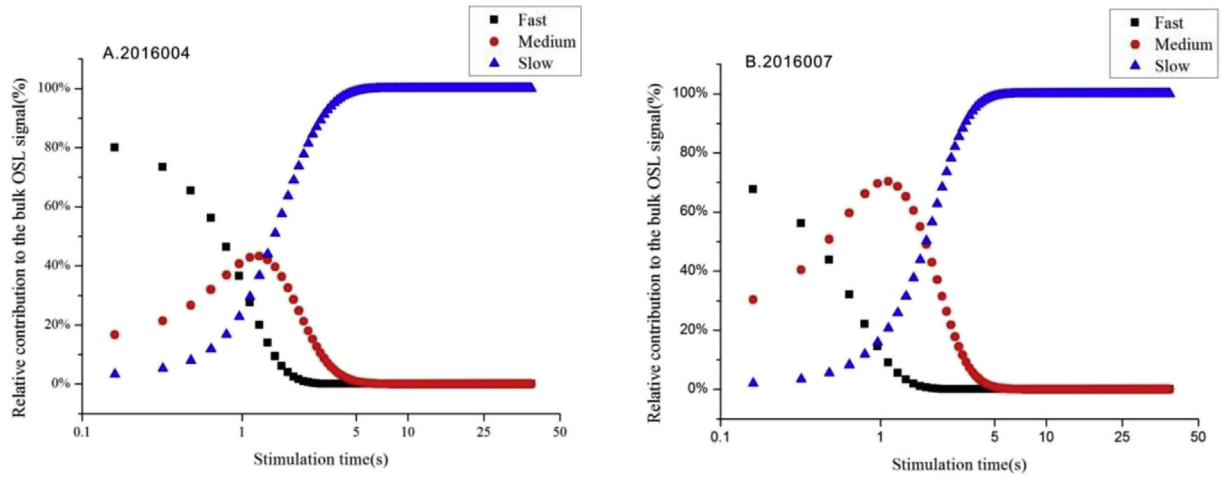

Fig. 5. Component separation of CW-OSL signals from natural quartz grains. The squares, circles, and triangles are the fast, medium, and slow components, respectively.

5. Discussion

5.1. Comparison between OSL and ^{14}C chronologies

The results of the OSL and AMS ^{14}C dating are shown in a depth-age model (Fig. 7).

Murray and Olley (2002) show broad agreement between ^{14}C and OSL ages, especially for aeolian sediment. This review was also verified in the current study, as OSL and ^{14}C ages, taken from the main Neolithic cultural stratum (Layers 4 and 5) where no traces of human activity was found in the upper layers, agreed well when compared and were both focused on the period from 4.0–3.3 ka. For instance, OSL samples 2016003, 2016008, and 2016009, collected from Layer 4, yielded ages of 3.38 ± 0.37, 3.38 ± 0.16, and 3.30 ± 0.16 ka, respectively. Those OSL ages were consistent with the corresponding ^{14}C ages, with resultant ages of 3593 ± 91 and 3589 ± 95 cal. BP, respectively.

The OSL ages and corresponding ^{14}C ages were reliable in the cultural accumulation (i.e. Layers 4 and 5), with the exception of Layer 3.

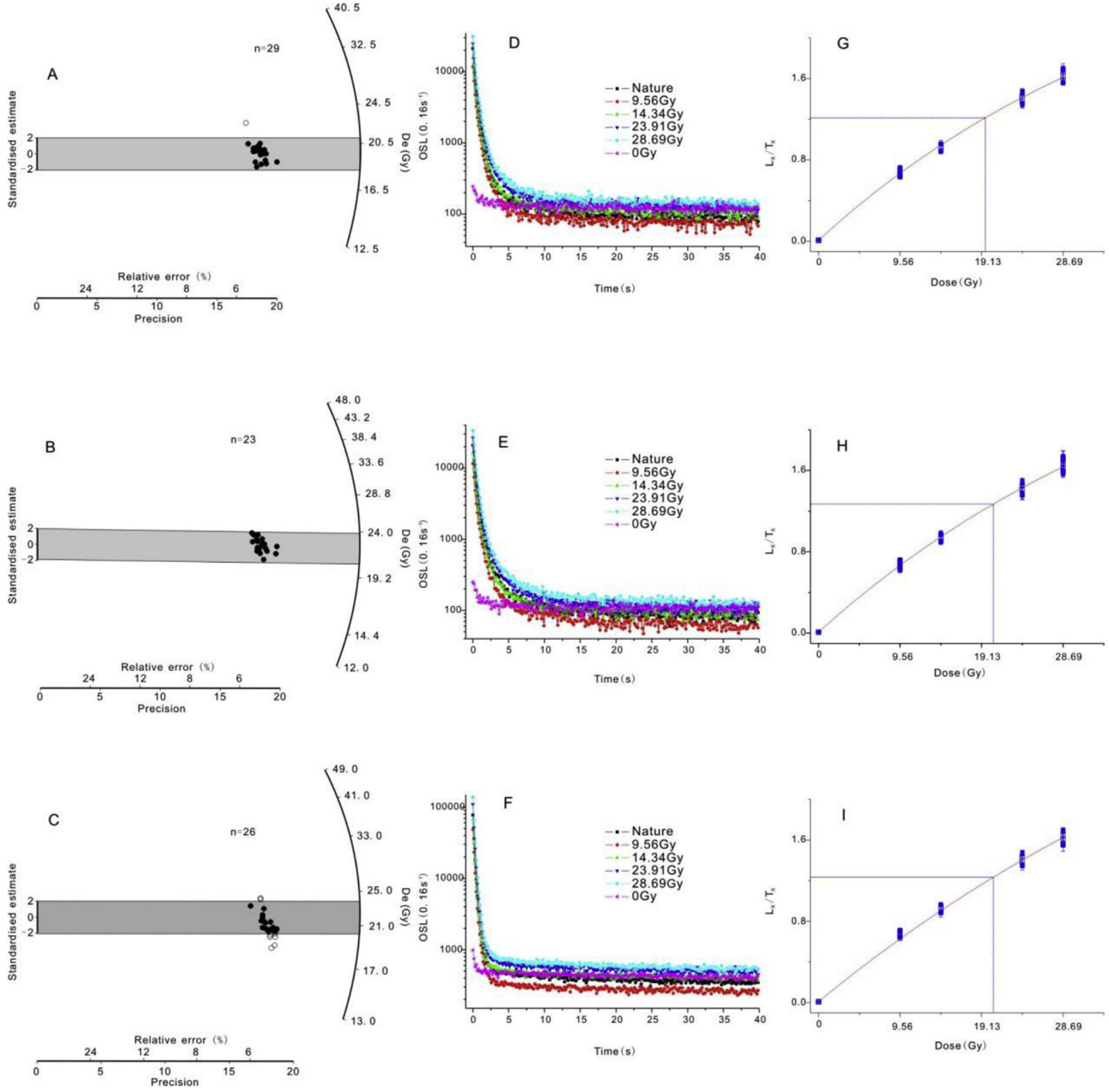

Fig. 6. Luminescence characteristics from medium-grained (38–63 μm) quartz for typical samples. They were 2016003 (A, D, and G), 2016004 (B, E, and H), and 2016009 (C, F, and I).

Table 2
Sample data and ^{14}C ages for the Neolithic site.

Lab code	Context No.	Sample type	Conventional radiocarbon age	Calibrated date (2σ range)
Beta-434875	Layer 3	Charcoal	3260 ± 30 BP	3484 ± 81 cal. BP
Beta-434876	Layer 4	Charcoal	3360 ± 30 BP	3593 ± 91 cal. BP
Beta-434877	Layer 5	Charcoal	3290 ± 30 BP	3516 ± 66 cal. BP
Beta-434878	Layer 5	Charcoal	3400 ± 30 BP	3644 ± 72 cal. BP
UGAMS#27094	Layer 3	Rice	3380 ± 25 BP	3641 ± 51 cal. BP
UGAMS#27093	Layer 4	Rice	3350 ± 25 BP	3589 ± 95 cal. BP
UGAMS#27092	Layer 5	Rice	3440 ± 25 BP	3729 ± 97 cal. BP

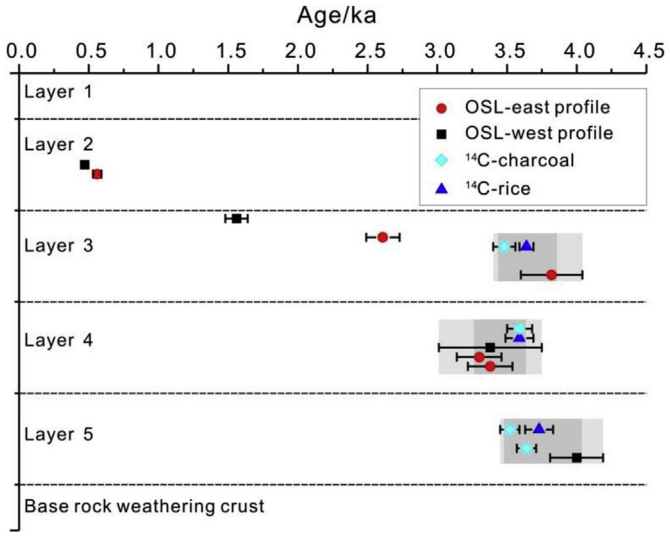

Fig. 7. Comparison between OSL (circle) and charcoal (triangle) ^{14}C dating results from different layers of the Pingfengshan site.

One of the OSL ages in Layer 3 agreed well with the corresponding ^{14}C age, while the two remaining OSL ages were consistently younger than the corresponding ^{14}C ages. In general, radiocarbon dating of charcoal or plant product samples is comparatively accurate due to the presence of unique organic carbon fractions, which have a definable ^{14}C activity, thereby indicating accurate ages. Thus, the ^{14}C ages obtained from charcoal and rice should not be underestimated or overestimated (Yu et al., 2016). The appearance of younger OSL ages (1.56 ± 0.08 and 2.61 ± 0.12 ka) in Layer 3 could be attributed to the sampling location and their relative stratigraphic relation. The thickness and deposition process of different settled layers could be affected by the slope and action of gravity. As shown in Fig. 2a and b, Layer 3 of the western profile had little shell accumulation, and the age, in theory, should be younger than the lower shell deposits of the eastern profile. Future work will need to distinguish the relative stratigraphic relation between Samples East 3–1 and East 3–2, which were not sampled using a sequence sampling method in a specific direction perpendicular to the stratigraphic profile.

The comparison between the OSL and ^{14}C ages confirmed that the OSL technique is reliable enough to record accurate depositional ages, especially when the ^{14}C age has limitations due to a lack of ^{14}C dating material or a reworking of sediment (Mischke et al., 2017; Zhang et al., 2012). Consequently, the combination of OSL and ^{14}C dating offers a better, high-resolution age control for the Pingfengshan site profiles for the past 4 ka. We believe that the OSL data represented the buried ages of the quartz grains, i.e. the ages of the buried stratigraphy, while the ^{14}C ages were more likely to indicate human activities. Post-depositional anthropogenic disturbances can have various influences on the determined OSL and ^{14}C ages. Cross-validation between different dating methods is crucial for chronology building in archaeological contexts.

5.2. Climatic conditions during the occupation of the Pingfengshan archaeological site

Based on the OSL dating and ^{14}C age of charcoal and rice, we determined that the type of culture at the Pingfengshan site pertained to the later stage of the Huangguashan culture (from 4.3–3.3 ka) along the northeast coast of Fujian Province (Fan et al., 2017). Twelve of the sixteen ages were distributed across the period from 4.0–3.3 ka (Fig. 8), especially near the 4.2 ka cold event, which represents an abrupt climate change that cooled or dried the climate with respect to the general climate trend during the Holocene. The archaeological sites in this region determined in previous studies were also concentrated between 4.3 and 3.3 ka. In order to understand the effect of sea level change and environmental conditions on human activity during the Huangguashan cultural period in Fujian Province, sea level change data for Fujian (Zeng, 1991) and the island of Taiwan (Zhang and Huang, 1996) and data on the strength of the Kuroshio (Jian et al., 2000) during the Holocene were used for comparison. The Kuroshio Current originates from the North Equatorial Current in the western Pacific, and transported warm and saline water flowing east of Taiwan and entering the Okinawa Trough towards the north. Its main axis is in the area of strongest heat exchange between ocean and atmosphere in the western Pacific, forcefully influencing the East Asian climate (Jian et al., 2000).

The spatial distribution of shell mounds was largely related to sea level fluctuation (Jin et al., 2017; Zhang and Huang, 1996). Relative sea level changes and the resulting palaeogeography can affect the rise and fall of settlement sites (Muru et al., 2017; Yue et al., 2015). Similar to the Jomon people (Yuan, 1995), the typical Neolithic culture of Japan, the Huangguashan people commonly adjusted their lifestyle to marine transgression and regression. Previous studies have shown that most living surfaces found in the shell mounds were located on the marine depositional terrace, the low platform of the estuary, and the coast in South China (Jin et al., 2017; Rolett et al., 2011). As shown in Fig. 8a, the sea level changes in Fujian (Zeng, 1991) and Taiwan (Zhang and Huang, 1996) showed a rising tendency during the period from 4.0–3.3 ka, with some slight differences. In the southern coastal area of the Yangtze Estuary, the abovementioned feature can potentially explain the difference in altitude distributions between the Huangguashan (approximately 50 m a.s.l.) and Pingfengshan sites (approximately 163 m a.s.l.). Notably, recent research has shown that the changes in numbers and spatiotemporal distribution of Neolithic sites were largely controlled by regional geomorphic evolution (particularly changes in the coast line) in coastal China (Yue et al., 2015). In addition, the regional geomorphic evolution was governed by sea level changes. The coastal plain (including the shelf) was largely submerged; only the foot of low hills to the west and southwest of the study area and islands protruding in the estuary fostered a limited number of settlements with characteristic maritime components, i.e. the thick-bedded shell accumulation horizon (Fig. 2).

Meanwhile, the coastal plain was vulnerable to extreme environmental events, which exerted great influence on the rise and fall of Neolithic culture (Rolett et al., 2011; Yue et al., 2015). Abrupt climate changes can cause large-scale human migrations or technical changes in agriculture (Ma et al., 2016; Muru et al., 2017). The sea surface temperature of Kuroshio (Jian et al., 2000), estimated by the planktonic foraminifera of Okinawa Trough sediments, can indirectly suggest strong or weak winter monsoons (Fig. 8b). The strong winter monsoon intervals indicated by the Okinawa foraminifera were related to cold events during the Holocene. We found that the cold events of 4.6 and 3.3 ka were closely related to the vicissitude of the Huangguashan culture, as shown in Fig. 8. In addition, it is clear that cold events during the recession of summer monsoons were common in the Asian and African monsoon regions (Wang et al., 2013). Therefore, the palaeoclimate of this area showed a weak winter monsoon and a strong summer monsoon for the duration of the Huangguashan culture. The fluctuant details of winter monsoon intensity during 4.6–3.3 ka showed that the climate conditions of the later stage of the Huangguashan culture (3.8–3.3 ka) were more suitable for human survival than those of the early stages (4.3–3.8 ka).

Because of abundant food resources and ascendant natural conditions, the developmental level of agriculture and stock farming in Fujian (subtropical area) was considerably below that of North China in the late Neolithic era (Gao and Pei, 2006). Climatic variation significantly influenced prehistoric human activities. The palaeoclimatic conditions of approximately 4.0 ka, which had lower sea levels and weaker winter monsoons, enlarged the onshore living area and promoted the agricultural industry. The appearance of rice agriculture (Deng et al., 2017) and cattle rearing (Wang et al., 2017) provides

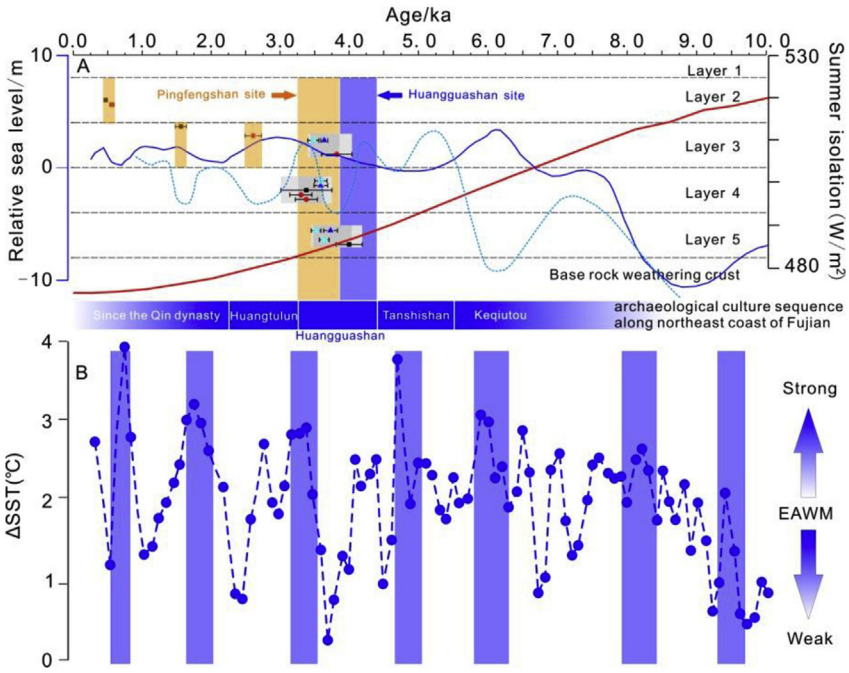

Fig. 8. Age distribution at the Pingfengshan site and the environmental background of the study area. (a) The red solid line represents the summer solar isolation at 30 °N (Berger and Loutre, 1991). The blue solid line represents the Holocene sea level change along the northeast coast of Fujian (Zeng, 1991), and the dashed line represents the sea level change along the coast of Taiwan, separated by the Taiwan Strait (Zhang and Huang, 1996). (b) The dashed line represents the strength of the Kuroshio Current, which is indicated by reconstructed sea surface temperature (SST) change gradients (Jian et al., 2000), and the shaded areas indicate North Atlantic cold events (Bond et al., 2001).

assertive evidence of the impact of climatic variation. At this period in time, with the climate turning colder and drier, the Huangguashan culture was clearly in decline. Cold-tolerant and drought-tolerant millet agriculture, indicated by the stable carbon isotope analysis of a pig jawbone excavated from the Pingfengshan site (Wang et al., 2017), was introduced into this area from North China at this time. Painted pottery, which flourished in the Huangguashan site, did not appear in the Pingfengshan site. A similar phenomenon of cultural recession occurred in vast areas of the middle and lower reaches of the Yellow River and Yangtze River (Nian et al., 2014). The 4.0 ka cold event exerted an important influence on the birth of the Sinic civilisation (Wu and Liu, 2004). The archaeological cultures all declined in about 2000 BC. For instance, the typical Longshan culture, which was characterised by delicate polished black pottery, was replaced by the Yueshi culture with coarse pottery (Zhang et al., 2010). The numbers of Yueshi cultural sites were less and the distribution range was smaller compared with those of Longshan cultural sites (Nian et al., 2014). The 3.3 ka cold event was one of the key factors that accelerated the recession of the Huangguashan culture, along with the spread of more advanced cultures from the lower reaches of the Minjiang River and the southern area of Zhejiang Province. The period of 3.25–2.75 ka is known as the Centuries of Darkness, and climate change could have been responsible for the global decline of empires of the Bronze Age (Nian et al., 2014; Wang et al., 2013). It was an era that saw the decline of the ancient Middle Kingdom of Egypt, Azov Empire, Hittite Old Kingdom, and Shang Dynasty of China (Wang et al., 2010).

The rise and fall of Neolithic culture in Fujian were not completely equivalent to those of the Yellow River Basin or Yangtze River Basin in China (Fan et al., 2017). Regional sea level changes played an important role in this area. In particular, sea level change could have affected onshore living space and site selection of prehistoric settlements, which led to a change in economic patterns during the Huangguashan cultural period. The intensive winter monsoon may have caused the recession of the Huangguashan culture, and the Huangguashan people were forced to abandon their settlement site due to colder and drier climatic conditions. In addition, cultures can shift to lower subsistence levels by reducing social complexity, abandoning human settlements, and reorganising systems of supply and production (DeMenocal, 2001). This could be the reason why the Huangguashan culture lasted for several centuries after the strong winter monsoon declined.

6. Conclusions

In this study, we showed that quartz OSL dating is a powerful tool for dating archaeological sites. The OSL ages of the Pingfengshan site (Layers 3–5) ranged from 4.00 ± 0.19 ka to 3.30 ± 0.16 ka. The ages obtained were reliable and consistent with the ^{14}C chronology. Both the OSL and radiocarbon ages were concentrated on the period from 4.0–3.3 ka. We believe that the OSL ages represented the buried ages of the quartz grains, i.e. the ages of the buried stratigraphy, while the ^{14}C ages were more likely to indicate human activity. Post-depositional anthropogenic disturbances can influence the OSL and ^{14}C ages in various ways. Cross-validation between different dating methods is crucial for chronology building in archaeological sites.

Climate change was the dominant influencing factor that caused the migration of prehistoric humans during the Huangguashan cultural period (4.3–3.2 ka). Sea level change could have affected onshore living space and site selection of prehistoric settlements, and the intensive winter monsoon likely contributed to the recession of the Huangguashan culture. The abrupt cold event of 3.3 ka was likely the key factor that accelerated the recession of the Huangguashan culture, along with the spread of more advanced cultures from the lower reaches of the Minjiang River and from the southern area of Zhejiang Province. Finally, the Huangguashan people were forced to abandon their settlement site due to colder and drier climatic conditions.

Acknowledgements

We thank the anonymous reviewers whose suggestions are cruvial for the revision of this paper. We are also grateful to Professor Thomas Higham for editing the manuscript. This research was financially supported by the Natural Science Foundation of Fujian Province (grant number 2018R1034-5),the Natural Science Foundation of China (grant numbers 41301012, 41771020, and U1405231) and Innovation Research Team Fund of Fujian Normal University (grant number IRTL1705).

Appendix A. Supplementary data

Supplementary data to this article can be found online at https://doi.org/10.1016/j.quageo.2018.10.001.

References

Aitken, M.J., 1998. An Introduction to Optical Dating: the Dating of Quaternary Sediments by the Use of Photon-stimulated Luminescence. Oxford University Press, Oxford 267 pp.

Berger, A., Loutre, M.F., 1991. Insolation values for the climate of the last 10 million years. Quat. Sci. Rev. 10, 297–317.

Bond, G., Kromer, B., Beer, J., Muscheler, R., Evans, M.N., Showers, W., Hoffmann, S., Lottibond, R., Hajdas, I., Bonani, G., 2001. Persistent solar influence on North Atlantic climate during the Holocene. Science 294 (5549), 2130–2136.

Chen, F., Dong, G., Zhang, D., Liu, X.Y., Jia, X., An, C.B., Ma, M.M., Xie, Y.W., Barton, L., Ren, X.Y., Zhao, Z.J., Wu, X.H., Jones, M.K., 2015. Agriculture facilitated permanent human occupation of the Tibetan Plateau after 3600 B.P. Science 347 (6219), 247–250.

ChongYi, E., Lai, Z., Hou, G., Cao, G., Sun, Y., Wang, Y., Jiang, Y., 2015. Age determination for a Neolithic site in northeastern Qinghai-Tibetan Plateau using a combined luminescence and radiocarbon dating. Quat. Geochronol. 30, 411–415.

DeMenocal, P.B., 2001. Cultural responses to climate change during the Late Holocene. Science 292, 667–673.

Deng, Z., Hung, H.-c., Fan, X., Huang, Y., Lu, H., 2017. The ancient dispersal of millets in southern China: new archaeological evidence. Holocene 28 (1), 34–43.

Fan, X., Huang, Y., Jin, J., Lei, X., Zhang, W., 2017. A brief introduction of Excavation at the Pingfengshan site in Xiapu county Fujian province. Fujian wenbo (1), 2–8.

Gao, X., Pei, S., 2006. An archaeological interpretation of ancient human lithic technology and adaptive strategies in China. Quat. Sci. 20 (4), 504–513.

Han, W., Yu, L., Lai, Z., Madsen, D., Yang, S., 2017. The earliest well-dated archeological site in the hyper-arid Tarim Basin and its implications for prehistoric human migration and climatic change. Quat. Res. 82 (01), 66–72.

Jian, Z., Wang, P., Saito, Y., Wang, J., Pflaumann, U., Oba, T., Cheng, X., 2000. Holocene variability of the Kuroshio current in the Okinawa Trough, northwestern pacific ocean. Earth Planet Sci. Lett. 184 (1), 305–319.

Jin, J., Li, Z., Huang, Y., Jiang, F., Fan, X., Ling, Z., Cheng, Y., Xu, X., 2017. Chronology of a late Neolithic Age site near the southern coastal region of Fujian, China. Holocene 27 (9), 1265–1272.

Jin, J., Li, Z., Jiang, F., Deng, T., Hu, F.g., Ling, Z., 2016. Coastal environment of the past millennium recorded by a coastal dune in Fujian, China. J. Arid Land 8 (5), 707–721.

Kitis, G., Vlachos, N.D., 2013. General semi-analytical expressions for TL, OSL and other luminescence stimulation modes derived from the OTOR model using the Lambert W-function. Radiat. Meas. 48, 47–54.

Lai, Z.P., Zöller, L., Fuchs, M., Brückner, H., 2008. Alpha efficiency determination for OSL of quartz extracted from Chinese loess. Radiat. Meas. 43 (2–6), 767–770.

Li, Z., Wu, X., Zhou, L., Liu, W., Gao, X., Nian, X., Trinkaus, E., 2017. Late Pleistocene archaic human crania from Xuchang, China. Science 355 (6328), 969–972.

Ma, T., Zheng, Z., Rolett, B.V., Lin, G., Zhang, G., Yue, Y., 2016. New evidence for Neolithic rice cultivation and Holocene environmental change in the Fuzhou Basin, southeast China. Veg. Hist. Archaeobot. 25 (4), 375–386.

Mischke, S., Liu, C., Zhang, J., Zhang, C., Zhang, H., Jiao, P., Plessen, B., 2017. The world's earliest Aral-Sea type disaster: the decline of the Loulan Kingdom in the Tarim Basin. Sci. Rep. 7, 43102.

Murray, A.S., Olley, J.M., 2002. Precision and accuracy in the optically stimulated luminescence dating of sedimentary quartz: a status review. Geochronometria 21.

Murray, A.S., Wintle, A.G., 2000. Luminescence dating of quartz using an improved single-aliquot regenerative-dose protocol. Radiat. Meas. 32 (1), 57–73.

Muru, M., Rosentau, A., Kriiska, A., Lougas, L., Kadakas, U., Vassiljev, J., Saarse, L., Aunap, R., Ku ttim, L., Puusepp, L., Kihno, K., 2017. Sea level changes and Neolithic hunter-Fisher-gatherers in the centre of Tallinn, southern coast of the Gulf of Finland, Baltic Sea. Holocene 27 (7), 917–928.

Nian, X., Chen, F., Li, F., Gao, X., 2015. Optical dating of a Paleolithic site near the eastern coastal region of Shandong, northern China. Quat. Geochronol. 30, 466–471.

Nian, X., Gao, X., Xie, F., Mei, H., Zhou, L., 2014. Chronology of the Youfang site and its implications for the emergence of microblade technology in North China. Quat. Int. 347, 113–121.

Olley, J.M., Caitcheon, G.G., Roberts, R.G., 1999. The origin of dose distributions in fluvial sediments, and the prospect of dating single grains from fluvial deposits using optically stimulated luminescence. Radiat. Meas. 30 (2), 207–217.

Reimer, P.J., Bard, E., Bayliss, A., Beck, J.W., Blackwell, P.G., Ramsey, C.B., Buck, C.E., Cheng, H., Edwards, R.L., Friedrich, M., 2013. IntCal13 and Marine13 radiocarbon age calibration curves 0? 50,000 Years cal BP. Radiocarbon 51, 1111–1150 4 (IntCal 13).

Rolett, B.V., Zheng, Z., Yue, Y., 2011. Holocene sea-level change and the emergence of neolithic seafaring in the fuzhou basin (fujian, China). Quat. Sci. Rev. 30 (7–8), 788–797.

Sun, Y., Chongyi, E., Lai, Z., Hou, G., 2017. Luminescence dating of prehistoric hearths in Northeast Qinghai Lake and its paleoclimatic implication. Archaeol. Anthropol. Sci. 10 (6), 1525–1534.

Wang, M., Ge, W., Huang, Y., Fan, X., 2017. C and N stable isotope analysis of pig bone from Pingfengshan shell mound. Sci. Conserv. Archaeol. 29 (5), 58–62.

Wang, S., Ge, Q., Wang, F., Wen, X., Huang, J., 2013. Abrupt climate changes of Holocene. Chin. Geogr. Sci. 23 (1), 1–12.

Wang, S., Wen, X., Huang, J., 2010. Global cooling in the immediate future? Chin. Sci. Bull. 55 (33), 3847–3852.

Wintle, A.G., Murray, A.S., 2006. A review of quartz optically stimulated luminescence characteristics and their relevance in single-aliquot regeneration dating protocols. Radiat. Meas. 41 (4), 369–391.

Wu, W., Liu, T., 2004. Possible role of the “Holocene event 3” on the collapse of neolithic cultures around the central plain of China. Quat. Int. 117 (1), 153–166.

Yu, L., An, P., Lai, Z., 2016. Different implications of OSL and radiocarbon ages in archaeological sites in the Qaidam Basin, Qinghai-Tibetan Plateau. Geochronometria 43 (1), 188–200.

Yuan, J., 1995. Study of the relationship between Jomon people and their environment based on shell mound. Adv. Earth Sci. 10 (4), 383–386.

Yue, Y., Zheng, Z., Rolett, B.V., Ma, T., Chen, C., Huang, K., Lin, G., Zhu, G., Cheddadi, R., 2015. Holocene vegetation, environment and anthropogenic influence in the Fuzhou Basin, southeast China. J. Asian Earth Sci. 99, 85–94.

Zeng, C., 1991. Sea level variation along Fujian coast in Holocene. J. Oceanogr. Taiwan Strait 10 (1), 77–84.

Zhang, G., Zhu, C., Wang, J., Zhu, G., Ma, C., Zheng, C., Zhao, L., Li, Z., Li, L., Jin, A., 2010. Environmental archaeology on longshan culture (4500–4000 aBP) at yuhuicun site in bengbu, anhui province. J. Geogr. Sci. 20 (3), 455–468.

Zhang, J.-F., Liu, C.-L., Wu, X.-H., Liu, K.-X., Zhou, L.-P., 2012. Optically stimulated luminescence and radiocarbon dating of sediments from Lop Nur (Lop Nor), China. Quat. Geochronol. 10, 150–155.

Zhang, W., Huang, Z., 1996. Holocene sea level changes along the coast of Taiwan. Trop. Geogr. 16 (3), 226–235.

Zheng, Y., Sun, G., Qin, L., Li, C., Wu, X., Chen, X., 2009. Rice fields and modes of rice cultivation between 5000 and 2500 BC in east China. J. Archaeol. 36 (12), 2609–2616.